Turk. J. Fish.& Aquat. Sci. 24(9), TRJFAS25612
https://doi.org/10.4194/TRJFAS25612

PROOF
RESEARCH PAPER

Turkish Journal of FISHERIES and AQUATIC SCIENCES

Macroalgal (*Ulva compressa*) Silver Nanoparticles: Their Characterization, Cytotoxicity, and Antibacterial Applications

Esra Armagan[1,*], Mukaddes Keskinates[2], Numan Emre Gumus[3], Ziya Aydin[4], Bahar Yilmaz[5], Mevlut Bayrakci[5]

[1]Karamanoglu Mehmetbey University, Ermenek Uysal and Hasan Kalan Health Services Vocational School, Department of Pharmacy Services, Karaman, Türkiye, 70400.
[2]Karamanoglu Mehmetbey University, Kazım Karabekir Vocational School, Department of Medical Services and Techniques, Karaman, Türkiye, 70100.
[3]Karamanoglu Mehmetbey University, Kazım Karabekir Vocational School, Department of Environmental Protection Technologies, Karaman, Türkiye, 70100.
[4]Karamanoglu Mehmetbey University, Vocational School of Technical Sciences, Karaman, Türkiye, 70100.
[5]Karamanoglu Mehmetbey University, Department of Bioengineering, Karaman, Türkiye, 70200

How to Cite

Armagan, E., Keskinates, M., Gumus, N.E., Aydin, Z., Yilmaz, B., Bayrakci, M. (2024). Macroalgal (*Ulva compressa*) Silver Nanoparticles: Their Characterization, Cytotoxicity, and Antibacterial Applications. *Turkish Journal of Fisheries and Aquatic Sciences*, *24(9)*, *TRJFAS25612.* https://doi.org/10.4194/TRJFAS25612

Article History
Received 18 February 2024
Accepted 11 June 2024
First Online 02 July 2024

Corresponding Author
E-mail: earmagan@kmu.edu.tr

Keywords
Silver nanoparticle
Algae
Green synthesis
Antibacterial effect
Cancer

Abstract

In this study, an extract of *Ulva compressa* (UC), a green macroalgae, was used to synthesize biogenic silver nanoparticles (AgNPs). The formation of nanoparticles (NPs) was evaluated and confirmed by using ultraviolet-visible (UV-VIS) spectroscopy, Fourier transform infrared spectroscopy (FT-IR), X-ray diffraction (XRD), and transmission electron microscopy (TEM) analyses. UV-VIS spectra showing absorption peaks at 450 nm confirmed the formation of AgNPs. The particles were crystalline in nature according to the XRD pattern. AgNPs formation was proved by the FT-IR spectrum of UC. TEM image showed that the average particle size was 4.55 nm. The antimicrobial and anticarcinogenic activity was evaluated for the synthesized AgNPs. AgNPs obtained from algae demonstrated antimicrobial activity against all bacteria including *B. subtilis, E. faecalis, S. mutans, E. coli, S. aureus*, and *S. pyogenes*. The NPs were shown to have anticarcinogenic activity on HEK 293, MCF-7, and HeLa (reducing viability by 25.42%, 46.42%, and 62.42%, respectively) cell cultures. These findings indicate that AgNPs can be useful medicinal compounds. Green synthesized NPs can be developed and utilized as anticancer agents in the treatment of various types of cancer, as well as their antimicrobial effects can be utilized to ensure the long-term sustainability of food in this study.

Introduction

The scientific interest in NPs is due to their small size (1-100 nm), which gives them new physical and chemical properties compared to their fine particles. As a result, they have been integrated into new applications in healthcare, food and feed, environmental care, cosmetics, optoelectronics, chemical, and biotechnology industries (Khatoon et al., 2017). Different types of NPs can be synthesized using numerous physical, chemical, biological, and hybrid methods. Although physical and chemical methods are the primary methods used to synthesize NPs, the use of toxic chemicals significantly reduces their biomedical applications, particularly in clinical areas (Li et al., 2011). The synthesis of NPs can be expensive, multi-step, and complex using current physical and chemical methods. These methods require high voltage, high temperature, and toxic solvents, and create residues and hazardous byproducts that have negative effects on biological applications and the environment (Ocsoy et al., 2018). Expanding their biomedical applications requires the

development of reliable, non-toxic, and environmentally friendly methods for NP synthesis (Li et al., 2011).

NPs can be made from different metals such as gold, nickel, selenium, iron, zinc, and silver (Ocsoy et al., 2018). NPs can be synthesized using biological methods with the use of bacteria, fungi, algae, plant extracts, enzymes, proteins, polysaccharides, or DNA (Chinnasamy et al., 2019). Targeted delivery, cancer therapy, gene therapy and DNA analysis, antibacterial agents, biosensors, and magnetic resonance imaging are just a few of the applications where biosynthesized NPs are utilized (Li et al., 2011).

Due to their many uses such as antioxidant, antibacterial, anti-angiogenic, wound healing, anti-inflammatory, and anticancer activity, AgNPs have become increasingly popular among metallic NPs in recent years (Rama et al., 2023). The properties of AgNPs that are optical, biomedical, catalytic, inhibitory, and bactericidal draw attention (Minhas et al., 2017). Studies have shown that AgNPs have antimicrobial properties by degrading enzymes, DNA damage, and inactivating cellular proteins (Nagmachi et al., 2022). Additionally, AgNPs have a huge surface area. As a result, it is more effective in interacting with microorganisms and exhibiting antimicrobial activity compared to other NPs (Chugh et al., 2021).

Algae are a group of organisms that are both economically and ecologically important. Medicine, pharmacy, forestry, aquaculture, and cosmetics are just some of the applications where they play a crucial role. Algae are used for the synthesis of NPs. Their high metal accumulation potential, ease of processing and cultivation, low-temperature growth, and low toxicness to the environment make them a good choice (Chugh et al., 2021). It is known that algae are rich in natural bioactive compounds (Minhas et al., 2017).

Therefore, UC was chosen to synthesize AgNPs in this study. The antibacterial properties of AgNPs synthesized were evaluated against various gram-negative and gram-positive bacterial species. Recently, AgNPs have also been successfully applied in the detection and treatment of cancer (Chugh et al., 2021). In this study, AgNPs made from green macroalgae were also examined for their anticarcinogenic effects on MCF-7, Hela, and HEK-293 cell lines.

Materials & Methods

Sample Collections

Green macroalgae UC (*L.*) *Kütz* seaweed was collected from Acıgol (Konya/Türkiye- 37°42’40” N, 33°39’38” E) Lake. Silver nitrate ($AgNO_3$), HEK 293 MCF-7 and Hela cancer cell lines, Dulbecco's Modified Eagle Medium (DMEM), Alamar Blue® reagent, streptococcal cultures (*B. subtilis*, *E. faecalis*, *S. mutans*, *E. coli*, *S. Aureus*, and *S. pyogenes*) in Mueller-Hinton (MH; US National Committee for Clinical Laboratory Standards (NCCLS)) were used in the study.

Preparation of UC Extract

The collected samples were washed thoroughly with tap and pure water to remove salt minerals, epiphytic organisms, and necrotic parts on the surface. The washed samples were dried in the shade for 7 days and then ground into powder for NP synthesis.

Synthesis of AgNPs

It was synthesized using a previously described method for green synthesis of AgNPs (Jahan et al., 2020). 5 g of dried algae extract (UC) was taken, mixed with 100 ml of distilled water heated to 100°C, and left for 20 minutes. Filtered through Whatman filter paper No. 1. The extract was collected and stored at 4°C, and then 90 ml of 1 mM $AgNO_3$ was prepared to synthesize AgNPs. For the synthesis of AgNPs, a 1 mM concentration of a filter-sterilized metal salt solution ($AgNO_3$) was used under optimum conditions. Synthesis was first monitored by visual color change. pH was adjusted between 10-11. Then, it was kept in a pressurized microwave (Sineo-MDS 10) at 60-70°C for 3 minutes. At the end of this, a color change was observed. Following the reduction of metal salts to NPs, NPs were purified by first centrifuging at 5000 rpm for 10 min and then at 18.000 rpm for 10 min. Its purpose is to remove large particles. The resulting NPs were washed thoroughly with distilled water to remove unconverted metal ions or any other reaction components. Then, the samples were first dried at -80°C and then freeze-dried into powder NPs and used for characterization.

Characterization of AgNPs

The green synthesis method used macroalgae extract to synthesize AgNPs, and they were characterized through UV-VIS spectroscopy, TEM and XRD, and the macroalgae extract was characterized through FT-IR. As the first step of the analysis, UV-VIS spectroscopy was used to prove the success of bioreduction of silver nitrate to AgNPs by aqueous extract of macroalgae and the resulting peaks were analyzed. FT-IR was performed using the Perkin Elmer Spectrum Two (Türkiye) device. FT-IR analysis was used to analyze the presence of functional groups and metabolites as well as to evaluate the agents present in AgNPs and their interaction with the macroalgae extract. The possible biomolecules were identified at a resolution of 4 cm^{-1} in the 4000-400 cm^{-1} range using an FT-IR spectrophotometer. Ulva extract and AgNPs were dried in an oven at 80°C. The dried materials were then ground into a fine powder and used for the recording of the spectra (González-Ballesteros et al., 2019). After the FT-IR step, XRD studies were carried out using the Rigaku Minifilex (Türkiye) device to confirm the crystal structure of AgNPs produced by UC. Biosynthesised AgNPs were dried and powdered for XRD analysis.

Analyzes were carried out at a speed of 2˚/min with a step interval of 0.02˚. X-rays were produced by operating the Cu Kα tube at 40 kV and 30 mA. As the last step to examine the morphological structure, TEM (JEOL 200 kV (Türkiye)) analysis was carried out. A solution containing AgNPs was prepared and dropped onto a carbon-coated copper grid to obtain the TEM micrograph. The formation of AgNPs was observed as a result of the characterization processes, and application studies were initiated.

Antibacterial Test (MIC)

In the investigation, AgNP solutions were tested for their antibacterial activity against bacteria gram-negative, such as *E. coli*, and gram-positive, such as *B. subtilis*, *S. aureus*, *S. mutans*, *E. faecalis*, and *S. pyogenes*. The microdilution method was used to determine the antibacterial activity using the minimum inhibitory concentration (MIC) (Bayat et al., 2023; Keskinkaya et al., 2023). Overnight, Mueller-Hinton's streptococcal cultures were adjusted to 106 colony-forming units (CFU/mL). Two serial dilutions of AgNP solutions in broth were prepared to achieve a final concentration of 0.125-5 mg/mL. The well that contained 100 µL of bacterial suspension was filled with 100 µL of each dilution of AgNP solutions in sterile 96-well plates. Triplicate samples were used to perform each test concentration. Negative controls were used to use wells that contained culture medium and bacteria. After 24 hours of incubation at 37˚C, turbidity measurements were taken for all wells. Using a microplate reader, the bacteria's growth at 600 nm was measured. As a result, the MIC at which reproduction was terminated was identified. MBC (minimum bacterial concentration) was defined as the lowest concentration of test compounds that prevented any visible bacterial growth on the Mueller-Hinton Agar (MHA) plate after 24 hours of incubation at 37˚C. In addition, chloramphenicol and ampicillin, which are commercial antibiotics, were utilized for comparison purposes.

Cytotoxicity Test

The Alamar Blue® assay was used to evaluate AgNPs' cytotoxicity on epithelial (HEK 293) and cancer cell lines (HeLa and MCF-7) by analyzing their cytotoxicity (Yilmaz et al., 2020; Yilmaz et al., 2022). Cells were grown in DMEM (4.5 g/L glucose; Gibco, Invitrogen, Karlsruhe Germany) medium at 37˚C in a 5% CO_2 atmosphere. Upon the growth of 10000 cells, they were gathered and placed in a 96-well cell culture plate. For 24 hours, the cells were incubated with 9 different doses of AgNPs, ranging from 0.1 µM to 1000 µM. The samples were prepared in triplicate. Only cells were used as negative control wells. For each concentration, media containing the test compounds were used and cells were incubated. Following 24 hours of incubation, the wells were filled with Alamar Blue® reagent (1:10, v/v) and left to incubate for 4 more hours. Spectrophotometric measurements were taken at 570 nm and 600 nm. Cell viability of each sample was calculated and control wells were taken as 100%. The expression for percent control is percent viability in the presence of tested compounds.

Results & Discussions

UV-VIS Spectrometry

The formation of AgNPs was visually observed by the appearance of a color change from slightly reddish to dark brown (Figure 1) in the reaction mixture (El-Kassas & El Komi, 2014). A sharp peak at 450 nm was observed in AgNPs by UV-VIS analysis. The formation of AgNPs was confirmed by the appearance of an

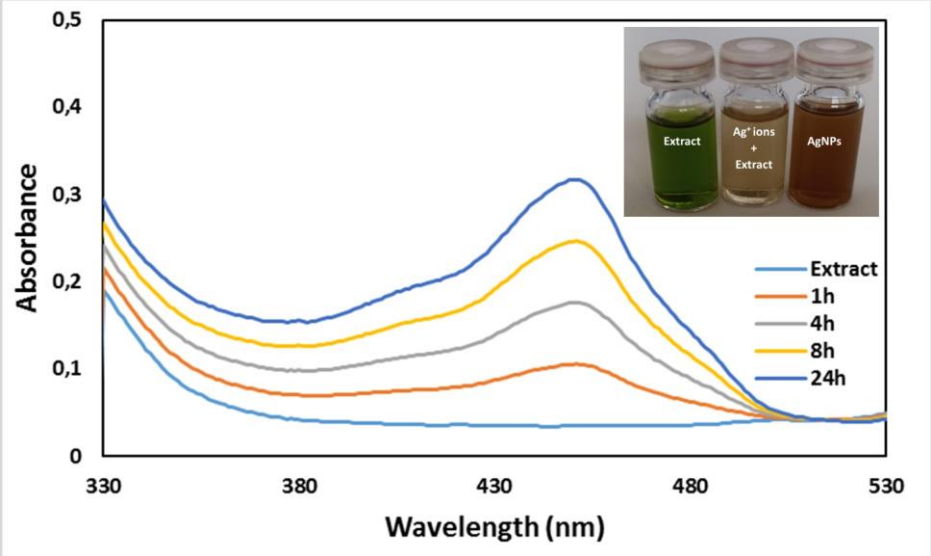

Figure 1. UV-VIS spectroscopy of AgNPs synthesized from green macroalgae at different time intervals and the inset image shows the colour change of the formation of AgNPs

absorption peak at 450 nm in UV-VIS spectroscopy (Figure 1). UV-VIS spectra were recorded periodically at different time intervals to monitor the conversion of AgNPs. After 24 hours, the difference in absorbance intensity levels was very small. It showed that the silver ions in the reaction mixture were reduced to metallic AgNPs. The characteristic absorption peak at 422 nm in the UV-VIS spectrum of green synthesised AgNPs using marine macroalgae *Chaetomorpha linum* confirmed the formation of AgNPs (Kannan et al., 2013). Another study reported that AgNPs synthesised green with *Chlorella vulgaris* gave a peak at 450 nm (the same wavelength as we obtained) in UV-VIS spectrometry (Soleimani & Habibi-Pirkoohi, 2017). Mohandoss et al. (2023) synthesized AgNPs using *Ulva lactuca* and obtained a maximum peak at 450 nm on spectral analysis. It has also been reported that the AgNPs obtained in the studies give peaks at different wavelengths due to synthesis under different reaction conditions. These different wavelengths could be due to varying NP sizes or varying capping agents of the extracts (González-Ballesteros et al., 2019).

FT-IR Analysis

The formation of UC-AgNPs is investigated through FT-IR spectroscopy by modifying and stretching vibrations of existing organic species (Hublikar et al., 2023). In the FT-IR technique, it can be seen that the functional groups of chemical components in the UC extract are what are responsible for reducing Ag^{+} ions into metallic AgNPs. Figure 2 shows the FT-IR spectra of the macroalgae extract used to form AgNPs. The FT-IR spectra of UC aqueous extract and UC-AgNPs showed peaks at different wavelengths corresponding to biomolecules involved in capping and bioreduction during the synthesis of these UC-AgNPs (Table 1). The FT-IR spectrum of UC extract showed major peaks at 3288 cm^{-1}, 1638 cm^{-1} and 1007 cm^{-1}, while the FT-IR spectra of biosynthesized UC-AgNPs exhibited three peaks at 3382 cm^{-1}, 1652 cm^{-1}, and 1096 cm^{-1} (Figure 2). The stretching band at 3382 cm^{-1} indicates the presence of either -OH groups from algal polysaccharides or -NH groups from amides (Minhas et al., 2017). However, this band is more intense and has a shift to a lower wave

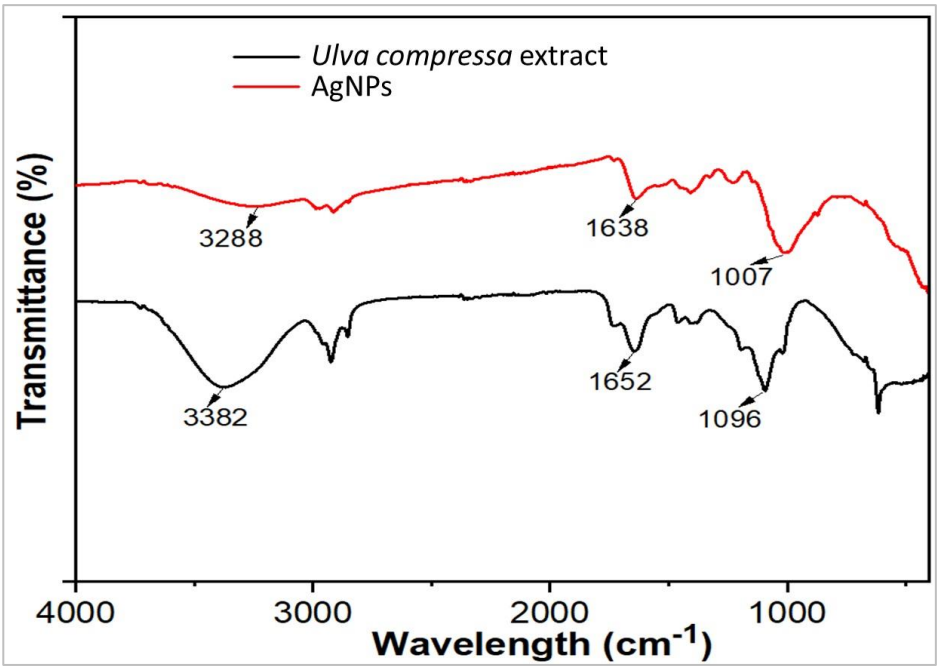

Figure 2. Fourier transform infrared spectroscopic data of AgNPs obtained from UC

Table 1. FTIR peaks and functional groups of UC extract and UC-AgNPs

UC Extract		UC-AgNPs	
FTIR peak (cm^{-1})	**Functional Group assigned**	**FTIR peak (cm^{-1})**	**Functional Group assigned**
3382	N–H stretch, O-H stretch, H-bonded	3288	N–H stretch, O-H stretch, H-bonded
2925	–C–H stretching	2907	–C–H stretching
1652	N–H bend	1638	N–H bend
1425	C-C stretching	1401	C-C stretching
1096	C-N stretching	1007	C-N stretching

number (3288 cm^{-1}) in the spectrum of AgNPs. Furthermore, the bending bands at 1652 $cm^{-1}$and 1096 cm^{-1} correspond to -NH groups of primary amines from the protein moiety and -CO groups of algal polysaccharides, respectively. These two bands are narrow and intense in the spectrum of AgNPs compared to the spectrum of the algal extract. The presence of N-H-bent primary amines is indicated by the narrow band at 1639 cm^{-1} (-NH-C=O) (Rajeshkumar et al., 2014).

XRD Analysis

The crystal structure of AgNPs produced with UC was confirmed by XRD studies after the FT-IR step. According to XRD analysis, these AgNPs possess a natural crystal structure. The pure silver structure can be identified by the intense diffraction peak at 2θ, which is located in the (220) plane. The characteristic planes (111), (200), and (220) of AgNPs, which have a face-centered cubic (FCC) structure, were observed at 38.06˚, 47.52˚, and 64.97˚, respectively (Figure 3). The purity of organic substances leads to other false fractions that are not outside the structure of pure silver. The XRD spectrum, Bragg peak position, and intensities were compared to standard JCPDS files (Ishak et al., 2020). The results were observed to have peaks at similar points with COD No: 9013418. The AgNPs synthesized in this study have a pure and crystalline structure, as confirmed by this study.

TEM Analysis

By using TEM, we examined the structure of AgNPs that were synthesized using the green method. In Figure 4, the TEM image of AgNPs synthesized from macroalgae extract is shown. The TEM image showed that the formed AgNPs were partially locally aggregated. AgNPs are susceptible to agglomeration due to their high free surface energy, which can be caused by the absence of support materials or bimetallic structures (Meng et al., 2022). The catalytic activity of AgNPs is influenced by the size, shape, and presence of support

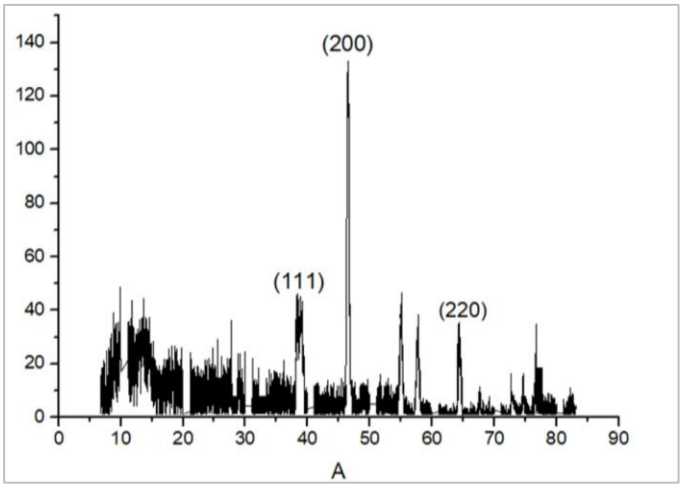

Figure 3. XRD patterns for AgNPs obtained by green synthesis

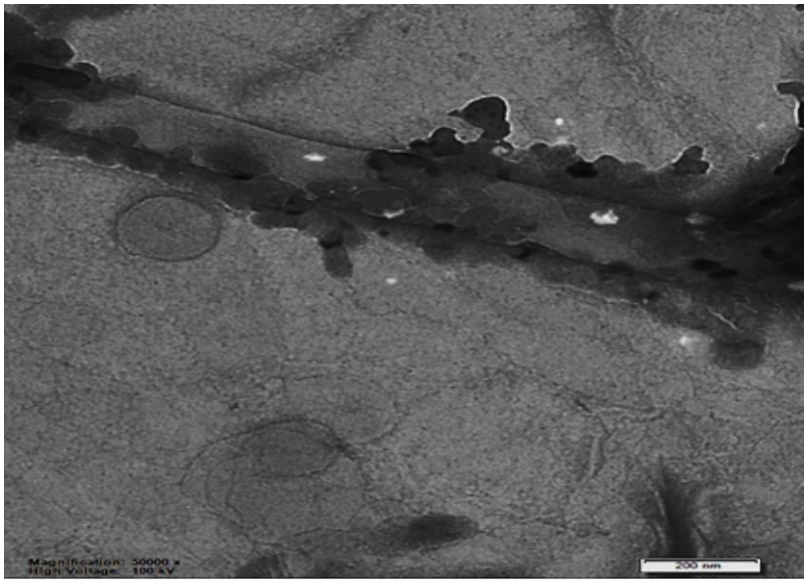

Figure 4. TEM image of AgNPs formed by green synthesis

material (Ren et al., 2020; Zhao et al., 2021). The study resulted in an average particle size of 4.55 nm. It is possible to say that this rate is quite comparable to the literature (Peng et al., 2012). The TEM images also showed a difference in the size and shape of the AgNPs compared to previously reported studies (Algotiml et al., 2022). TEM image of AgNPs synthesised by marine the red alga *Spyridia fusiformis* showed NPs in the size range of 5-50 nm (Murugesan et al., 2017). In another study, the size of AgNPs from marine macroalgae was interpreted to be between 2 and 35 nm in a TEM analysis (Vinayagam et al., 2024). The different algal species collected under different environmental conditions at the sampling sites in the oceans may explain this result (Algotiml et al., 2022).

AgNPs Exhibit Antimicrobial Activity

The microdilution method was used to examine the antibacterial properties of AgNPs against *B. subtilis*, *S. aureus*, *S. mutans*, *E. coli*, *S. pyogenes*, and *E. faecalis*. Table 2 shows the results of bacterial growth obtained from the antibacterial test. All examined marine macroalgae extracts were found to have antibacterial effects on all test pathogens at different concentrations. In particular, AgNPs showed superior antibacterial activity against *B. subtilis* (MIC: 4.35 mg/mL) and *S. mutans* (MIC: 3.5 mg/mL). AgNPs were antibacterial against both gram-negative and gram-positive bacteria, but more effective against gram-positive bacteria. The difference in cell wall thickness between gram-positive and gram-negative bacteria may be another reason for the different antimicrobial activity of AgNPs against pathogens (Chatterjee et al., 2015). Antibacterial activity can also be influenced by factors such as size, shape, concentration, time and charge of the AgNPs (Raza et al., 2016).

AgNPs Have Cytotoxic Effects

AgNPs play an effective role in the treatment of various types of cancer, particularly lung, cervical and breast cancer (Algotiml et al., 2022). Epithelial (HEK 293) and cancer cell lines (MCF-7 and HeLa) were tested for AgNPs' cytotoxicity using the Alamar Blue® assay. The viability results and images of cells obtained from cytotoxicity tests are shown in Figure 5 and 6. The study revealed that there was a decrease in viability due to an increase in AgNP concentration at different concentrations (0-1000 µg/mL). The anticancer activity of the biosynthesised AgNPs was found to be dose-dependent. Cell viability decreased progressively with increase in AgNP concentration. When 1000 µg/mL AgNPs were used, there was a decrease in viability of 25.42%, 46.42%, and 62.42% in HEK 293, MCF-7, and HeLa cells, respectively. AgNPs, which displayed high cytotoxicity, particularly on the cancer cell line, resulted in lower cytotoxicity in the epithelial cell. Green synthesized AgNPs were found to be more sensitive to cancer cells in cytotoxicity results. There are studies that have reported that AgNPs synthesised by other algae species (*Ulva lactuca, Cystoseira myrica*) have a strong cytotoxic effect on the MCF-7 cell line (Devi & Valentin, 2012; Mohamed et al., 2022).

Conclusion

The characterization studies revealed that the NPs were synthesized with an average size of 4.55 nm and a pure and crystalline structure. The microdilution method showed that AgNPs had antibacterial properties against both gram-negative and gram-positive bacteria, with a stronger response against gram-positive bacteria. The synthesized AgNPs were tested for their anticancer ability on HEK 293, MCF-7, and HeLa cell lines. AgNPs were observed to have an anticarcinogenic effect and exhibited a higher activation, particularly on cancer cell lines. According to the findings, the green macroalgae (*Ulva compressa*) utilized in NP synthesis may be a valuable resource for the creation of non-toxic anticancer and antimicrobial agents in the future.

Ethical Statement

This study does not require any formal authorization. The authors declare that the present study was conducted in an ethical, professional, and responsible manner.

Funding Information

No funding was received for conducting this study.

Author Contribution

All authors contributed to the study conception and design. Material preparation, data collection and analysis were performed by Bahar Yilmaz, Mukaddes

Table 2. Minimum inhibitory concentration (MIC) of AgNPs

	MIC (mg/mL)		
	AgNPs	*Chloramphenicol*	*Ampicillin*
B. subtilis	4.35	3.75	5.25
E. faecalis	5.5	1.25	0.75
S. mutans	3.5	3.75	1.75
E. coli	4.75	5	4.25
S. aureus	5.25	3.75	2.5
S. pyogenes	8.5	1.25	2

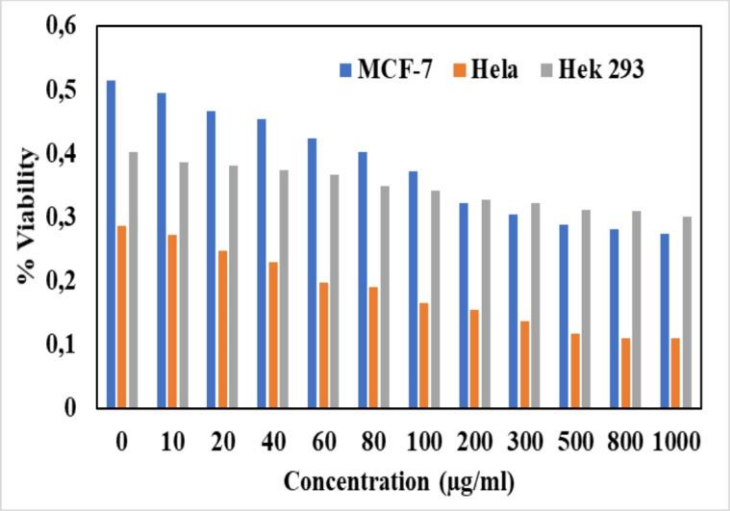

Figure 5. In vitro cytotoxicity results on different cells for AgNPs catalyst obtained by green synthesis

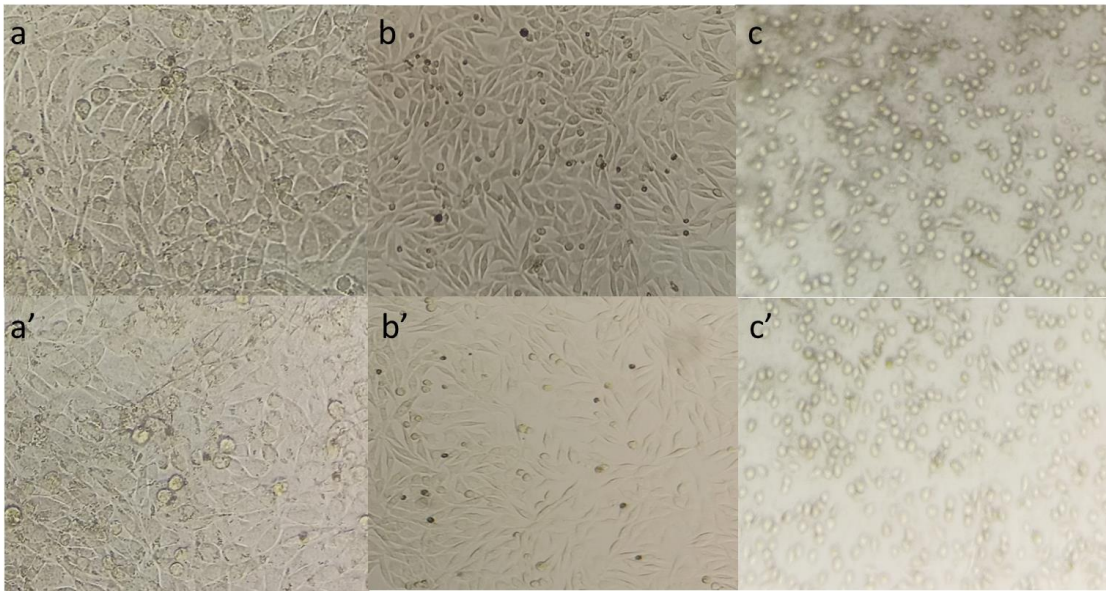

Figure 6. Cytotoxicity of the synthesized AgNPs from UC extract (a: MCF-7 untreated control cell lines, a': MCF-7 cell lines treated by AgNPs, b: HeLa untreated control cell lines, b': HeLa cell lines treated by AgNPs, c: HEK 293 untreated control cell lines, c': HEK 293 cell lines treated by AgNPs)

Keskinates and Numan Emre Gumus. EA: investigation, methodology, data curation, and writing original draft. MK: investigation, methodology, data curation, and writing original draft. NEG: investigation, methodology, data curation, and writing original draft. ZA: investigation, methodology, data curation, writing original draft, and validation. BY: investigation, methodology, data curation, writing original draft, and validation. MB: investigation, methodology, data curation, writing original draft, and validation. All authors read and approved the final manuscript.

Conflict of Interest

The authors declare that they have no known competing financial or non-financial, professional, or personal conflicts that could have appeared to influence the work reported in this paper.

References

Algotiml, R., Gab-Alla, A., & Seoudi, R. (2022). Anticancer and antimicrobial activity of biosynthesized Red Sea marine algal silver nanoparticles. *Scientific Reports*, 2421. https://doi.org/10.1038/s41598-022-06412-3

Bayat, R., Akin, M., & Yilmaz, B. (2023). Biogenic platinum based nanoparticles: synthesis, characterization and their applications for cell cytotoxic, antibacterial effect, and direct alcohol fuel cells. *Chemical Engineering Journal Advances*, 14. https://doi.org/10.1016/j.ceja.2023.100471

Chatterjee, T., Chatterjee, B. K., & Majumdar, D. (2015). Antibacterial effect of silver nanoparticles and the modeling of bacterial growth kinetics using a modified Gompertz model. *Biochimica et Biophysica Acta*, 1850, 299–306. https://doi.org/10.1016/j.bbagen.2014.10.022

Chinnasamy, G., Chandrasekharan, S., & Bhatnagar, S. (2019).

Biosynthesis of silver nanoparticles from *Melia azedarach*: enhancement of antibacterial, wound healing, antidiabetic and antioxidant activities. *International Journal of Nanomedicine*, 14, 9823–9836. https://doi.org/10.2147/IJN.S231340

Chugh, D., Viswamalya, V. S., & Das, B. (2021). Green synthesis of silver nanoparticles with algae and the importance of capping agents in the process. *Journal of Genetic Engineering and Biotechnology*, 19, 126. https://doi.org/10.1186/s43141-021-00228-w

Devi, J. S., & Valentin, B. (2012). Anticancer Activity of silver nanoparticles synthesized by the seaweed *Ulva lactuca in vitro*. *Open Access Scientific Reports*, 1:4. http://dx.doi.org/10.4172/scientificreports.242

El-Kassas, H., & El Komi, M. M. (2014). Biogenic silver nanoparticles using seaweed *Ulva rigida* and their fungicidal and cytotoxic effects. *Journal of King Abdulaziz University,* 25, 3–20. https://doi.org/10.4197/mar.25.1

González-Ballesteros, N., Rodríguez-Argüelles, M. C., & Prado-López, S. (2019). Macroalgae to nanoparticles: Study of *Ulva lactuca* L. role in biosynthesis of gold and silver nanoparticles and of their cytotoxicity on colon cancer cell lines. *Materials Science & Engineering C*, 97, 498–509. https://doi.org/10.1016/j.msec.2018.12.066

Hublikar, L. V., Ganachari, S. V., & Patil, V. B. (2023). Anticancer potential of biologically synthesized silver nanoparticles using *Lantana camara* leaf extract. *Progress in biomaterials*, 12, 155–169. https://doi.org/10.1007/s40204-023-00219-9

Ishak, NAIM, Kamarudin, S. K., & Timmiati S. N. (2020). Biogenic platinum from agricultural wastes extract for improved methanol oxidation reaction in direct methanol fuel cell. *Journal of Advanced Research*, 28, 63–75. https://doi.org/10.1016/j.jare.2020.06.025

Jahan, I., Erci, F., & Koc Cakir, R. (2020). Microwave-irradiated green synthesis of metallic silver and copper nanoparticles using fresh ginger (*Zingiber officinale*) rhizome extract and evaluation of their antibacterial potentials and cytotoxicity. *Inorganic and Nano-Metal Chemistry*, 51, 722–732. https://doi.org/10.1080/24701556.2020.1808017

Kannan, R. R. R., Arumugam, R., & Ramya, D. (2013). Green synthesis of silver nanoparticles using marine macroalga *Chaetomorpha linum*. *Applied Nanoscience*, 3, 229–233. https://doi.org/10.1007/s13204-012-0125-5

Keskinkaya, H. B., Deveci, E., & Altinok Yilmaz, B. (2023). HPLC-UV analysis of phenolic compounds and biological activities of *Padina pavonica* and *Zanardinia typus* marine macroalgae species. *Turkish Journal of Botany*, 47, 231–243. https://doi.org/10.55730/1300-008X.2761

Khatoon, N., Mazumder, J. A, & Sardar, M. (2017). Biotechnological applications of green synthesized silver nanoparticles. *Journal of Nanosciences: Current Research*, 2:1. DOI:10.4172/2572-0813.1000107

Li, X., Xu, H., & Chen, Z. S. (2011). Biosynthesis of nanoparticles by microorganisms and their applications. *Journal of Nanomaterials*, 8, 1–16. https://doi.org/10.1155/2011/270974

Meng, W., He, H., & Yang, L. (2022). 1D-2D hybridization: nanoarchitectonics for grain boundary-rich platinum nanowires coupled with MXene nanosheets as efficient methanol oxidation electrocatalysts. *Chemical Engineering Journal*, 450:137932. https://doi.org/10.1016/j.cej.2022.137932

Minhas, F. T., Arslan, G., & Gubbuk, I.H. (2017). Evaluation of antibacterial properties on polysulfone composite membranes using synthesized biogenic silver nanoparticles with *Ulva compressa* (L.) Kütz. and *Cladophora glomerata* (L.) Kütz. extracts. *International Journal of Biological Macromolecules,* 107, 157–165. https://doi.org/10.1016/j.ijbiomac.2017.08.149

Mohamed, R. M., Fawzy, E. M., & Shehab, R. A. (2022). Production, characterization, and cytotoxicity effects of silver nanoparticles from brown alga (*Cystoseira myrica*). *Journal of Nanotechnology,* 2022. https://doi.org/10.1155/2022/6469090

Mohandoss, S., Murugaboopathy, V., & Haricharan, P. B. (2023). Ulvan as a reducing agent for the green synthesis of silver nanoparticles: a novel mouthwash. *Inorganics*, 11(1), 5. https://doi.org/10.3390/inorganics11010005

Murugesan, S., Bhuvaneswari, S., & Sivamurugan, V. (2017). Green synthesis, characterization of silver nanoparticles of a marine red alga *Spyridia fusiformis* and their antibacterial activity. *International Journal of Pharmacy and Pharmaceutical Sciences*, 9, 192–197. http://dx.doi.org/10.22159/ijpps.2017v9i5.17105

Naghmachi, M., Raissi, A., & Baziyar, P. (2022). Green synthesis of silver nanoparticles (AgNPs) by *Pistacia terebinthus* extract: Comprehensive evaluation of antimicrobial, antioxidant and anticancer effects. *Biochemical and Biophysical Research Communications*, 608, 163–169. https://doi.org/10.1016/j.bbrc.2022.04.003

Ocsoy, I., Tasdemir, D., & Mazicioglu, S. (2018). Nanotechnology in plants. *Advances in Biochemical Engineering/Biotechnology*, 164, 263–275. https://doi.org/10.1007/10_2017_53

Peng, Z., Somodi, F., & Helveg, S. (2012). High-resolution in situ and ex situ TEM studies on graphene formation and growth on Pt nanoparticles. *Journal of Catalysis*, 286, 22–29. https://doi.org/10.1016/j.jcat.2011.10.008

Rajeshkumar, S., Malarkodi, C., & Paulkumar, K. (2014). Algae mediated green fabrication of silver nanoparticles and examination of its antifungal activity against clinical pathogens. *International Journal of Metalcasting*, 2014, 1–8. https://doi.org/10.1155/2014/692643

Rama, P., Mariselvi, P., & Sundaram, R. (2023). Eco-friendly green synthesis of silver nanoparticles from *Aegle marmelos* leaf extract and their antimicrobial, antioxidant, anticancer and photocatalytic degradation activity. *Heliyon*, 9:e16277. https://doi.org/10.1016/j.heliyon.2023.e16277

Raza, M. A., Kanwal, Z., & Rauf, A. (2016). Size- and shape-dependent antibacterial studies of silver nanoparticles synthesized by wet chemical routes. *Nanomaterials*, 6:74. https://doi.org/10.3390/nano6040074

Ren, X., Lv, Q., & Liu, L. (2020). Current progress of Pt and Pt-based electrocatalysts used for fuel cells. *Sustainable Energy Fuels*, 4, 15–30. DOI: 10.1039/C9SE00460B

Soleimani, M., & Habibi-Pirkoohi, M. (2017). Biosynthesis of silver nanoparticles using *Chlorella vulgaris* and evaluation of the antibacterial efficacy against *Staphylococcus aureus*. *Avicenna Journal of Medical Biotechnology*, 9, 120–125.

Vinayagam, R., Nagendran, V., & Goveas, L. C. (2024). Structural characterization of marine macroalgae derived silver nanoparticles and their colorimetric sensing of hydrogen peroxide. *Materials Chemistry and Physics*, 313. https://doi.org/10.1016/j.matchemphys.2023.128787

Yilmaz, B. (2022). Release of nifedipine, furosemide, and

niclosamide drugs from the biocompatible poly(HEMA) hydrogel structures. *Turkish Journal of Chemistry*, 46, 1710–1722. https://doi.org/10.55730/1300-0527.3474

Yilmaz, B., Bayrac, A. T., & Bayrakci, M. (2020). Evaluation of anticancer activities of novel facile synthesized calix[n]arene sulfonamide analogs. *Applied biochemistry and biotechnology*, 190, 1484–1497. https://doi.org/10.1007/s12010-019-03184-x

Zhao, G., Fang, C., & Hu, J. (2021). Platinum-based electrocatalysts for direct alcohol fuel cells: enhanced performances toward alcohol oxidation reactions. *Chempluschem*, 86, 574–586. https://doi.org/10.1002/cplu.202000811